Expression of Spinach Glycolate Oxidase in *Saccharomyces cerevisiae*: Purification and Characterization†

Peter Macheroux, Vincent Massey,* and Dennis J. Thiele
Department of Biological Chemistry, University of Michigan Medical School, Ann Arbor, Michigan 48109-0606
Micha Volokita
MSU-DOE Plant Research Laboratory, Michigan State University, East Lansing, Michigan 48824
Received December 11, 1990; Revised Manuscript Received February 8, 1991

ABSTRACT: Glycolate oxidase from spinach has been expressed in *Saccharomyces cerevisiae*. The active enzyme was purified to near-homogeneity (purification factor ~1400-fold) by means of hydroxyapatite and anion-exchange chromatography. The purified glycolate oxidase is nonfluorescent and has absorbance peaks at 448 (ϵ = 9200 M^{-1} cm^{-1}) and 346 nm in 0.1 M phosphate buffer, pH 8.3. The large bathochromic shift of the near-UV band indicates that the N(3) position is deprotonated at pH 8.3. A pH titration revealed that the pK of the N(3) is shifted from 10.3 in free flavin to 6.4 in glycolate oxidase. Glycolate oxidase is competitively inhibited by oxalate with a K_d of 0.24 mM at 4 °C in 0.1 M phosphate buffer, pH 8.3. Three pieces of evidence demonstrate that glycolate oxidase stabilizes a negative charge at the N(1)–C(2=O) locus: the enzyme forms a tight sulfite complex with a K_d of 2.7 × 10^{-7} M and stabilizes the anionic flavosemiquinone and the benzoquinoid form of 8-mercapto-FMN. Steady-state analysis at pH 8.3, 4 °C, yielded a K_m = 1 × 10^{-3} M for glycolate and K_m = 2.1 × 10^{-4} M for oxygen. The turnover number has been determined to be 20 s^{-1}. Stopped-flow studies of the reductive (k = 25 s^{-1}) and oxidative (k = 8.5 × 10^4 M^{-1} s^{-1}) half-reactions have identified the reduction of glycolate oxidase to be the rate-limiting step.

Glycolate oxidase (EC 1.1.3.1) is a flavoprotein catalyzing the oxidation of α-hydroxy acids to the corresponding α-keto acids:

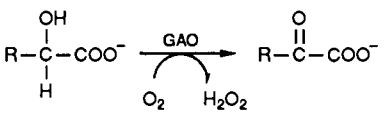

The highest affinity was found for glycolate (R = H) followed by L-lactate (R = CH_3). Glyoxylate, which is the product of glycolate oxidation, is also oxidized by the enzyme, yielding oxalate. Studies with the enzyme from pea leaves demonstrated the high stereospecificity for the *re* hydrogen (>99.7%) when the prochiral glycolate is used as a substrate. Glycolate oxidase is found in the peroxisomes of liver tissue of vertebrates (Schuman & Massey, 1971; Schwam et al., 1979) as well as in many plants (Tolbert et al., 1949; Zelitch & Ochoa, 1953; Kerr & Groves, 1975; Nishimura et al., 1983) where the enzyme plays a crucial role in photorespiration.

The primary structure of glycolate oxidase from spinach has been determined by peptide sequencing (Cederlund et al., 1988) and also has been deduced from the DNA sequence of a cDNA clone (Volokita & Somerville, 1987). The three-dimensional structure has been elucidated by X-ray crystallography and is available at 2.0-Å resolution (Lindqvist, 1989). The knowledge of the amino acids in the active site, i.e., near the flavin mononucleotide (FMN)[1] ring system, provides the necessary background for the study of the role of each amino acid in catalysis.

Flavoprotein oxidases have a few properties in common which are not found in other flavoproteins, such as formation of sulfite adducts and stabilization of anionic flavin semiquinones and the benzoquinoid form of 8-mercaptoflavin [for a review, see Ghisla and Massey (1986)]. It is generally accepted that these characteristic features are related to a very specific amino acid environment, such as a positively charged amino acid close to the N(1)–C(2=O) locus. The purpose of our investigation is to further substantiate the involvement of certain amino acids, like the lysine near the N(1)–C(2=O), by replacement with a "nonfunctional" amino acid employing active-site-directed mutagenesis.

Since little information on spinach glycolate oxidase is available with regard to its properties, our first goal was to establish that glycolate oxidase behaves like a typical member of this class of flavoproteins, as can be expected from the crystal structure. In order to investigate the role of some of the amino acids in the active site, as discussed above, we expressed the enzyme in yeast cells transformed with a plasmid carrying the cDNA of spinach glycolate oxidase. In this paper, we describe the purification, characterization, and properties of wild-type glycolate oxidase isolated from yeast cells.

Materials and Methods

Materials. Glycolic acid, iodoacetamide, and methyl methanethiosulfonate (MMTS) were purchased from Aldrich. Horseradish peroxidase, *o*-dianisidine, glyoxylic acid, FMN, phenylmethanesulfonyl fluoride (PMSF), D-(+)-glucose, and all amino acids were purchased from Sigma. Yeast nitrogen base without amino acids was from Difco Laboratories, Detroit, MI. 8-Mercapto-FMN was freshly prepared from 8-chloro-FMN as described in the literature (Massey et al., 1979).

Enzyme Assay. Glycolate oxidase activity was measured in an enzyme-coupled assay using horseradish peroxidase and *o*-dianisidine to remove hydrogen peroxide generated during oxidation of glycolate. A typical assay mixture contained 10 μL of horseradish peroxidase (1 mg/mL), 50 μL of *o*-di-

† This work was supported by a grant from the U.S. Public Health Service (NIH Grant GM-11106) to V.M. and by a Feodor-Lynen Fellowship of the Alexander von Humboldt Foundation to P.M.
* Author to whom correspondence should be addressed.

[1] Abbreviations: MMTS, methyl methanethiolsulfonate; EDTA, ethylenediaminetetraacetic acid; PMSF, phenylmethanesulfonyl fluoride; FMN, flavin mononucleotide; TN, turnover number.

0006-2960/91/0430-4612$02.50/0

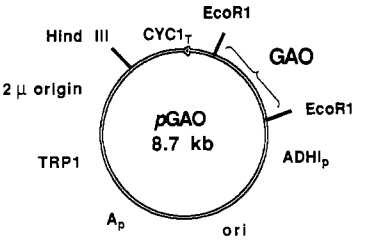

FIGURE 1: Vector *p*GAO used for expression of glycolate oxidase in yeast. The plasmid contains the promoter from the yeast alcohol dehydrogenase I gene ($ADHI_p$), the transcription termination signal from the yeast iso-1-cytochrome *c* gene ($CYC1_T$), the 2 μ origin allowing replication of the plasmid in yeast, a selectable gene for introduction and maintenance of the plasmid in yeast (TRP1), the ampicillin resistance gene for selection in *E. coli* (A_p), an origin of replication for propagation in *E. coli* (ori), and eventually the glycolate oxidase sequence (GAO) inserted into an *Eco*RI restriction site.

anisidine solution (8 mM, 20% Triton X-100), 10 μL of sodium glycolate (1 M), and 930 μL of 0.1 M potassium phosphate buffer, pH 8.3. The reaction was started by adding 10 μL of the glycolate oxidase sample. Formation of the *o*-dianisidine radical cation which reflects the catalytic activity of glycolate oxidase was monitored at 440 nm and at 25 °C (ϵ_{440} = 11 600 M^{-1} cm^{-1}).

Expression of Spinach Glycolate Oxidase in Saccharomyces cerevisiae. An expression vector based on the strong, constitutively active yeast alcohol dehydrogenase I (*ADHI*) promoter (Ammerer, 1983) was constructed for the purification of glycolate oxidase. A *Dra*I restriction enzyme site 17 nucleotides 5′ to the glycolate oxidase initiation codon in the cDNA (Volokita & Somerville, 1987) was cleaved, and *Eco*RI linkers were added by T4 DNA ligase (Maniatis et al., 1982). The 1.4-kb *Eco*RI DNA fragment encompassing the entire glycolate oxidase open reading frame was inserted in the *Eco*RI site of plasmid *p*YCDE-2, a derivative of *p*MAC561 (McKnight & McConaughy, 1983), with the 5′ end of the cDNA adjacent to the *ADHI* promoter sequence. The authenticity of the resultant plasmid, denoted *p*GAO (Figure 1), was verified by standard restriction endonuclease mapping (Maniatis et al., 1982). Plasmid *p*GAO was introduced into yeast strain DTY3 (*MATα trp-1 leu2-3 Leu2-112 gal1 ura3-50 his cup1*^{s}; Thiele et al., 1986) by the lithium acetate transformation procedure (Ito et al., 1983), and transformants were selected on synthetic complete medium lacking tryptophan (SC-trp) as described (Sherman et al., 1983). Single colonies were purified on SC-trp agar and used to inoculate liquid starter cultures for the fermentor.

Growth of S. cerevisiae. Cells were first grown on a small scale (100 mL and 1 L, respectively), and a total of 4 L of stationary-phase culture was used to inoculate 180 L of the same medium (New Brunswick fermentor). The growth temperature was 30 °C, and the pH was maintained at 5.9. Under these conditions, the cells have a generation time of 2.5 h. The growth of the culture was monitored spectrophotometrically, and harvest with a Sharples continuous centrifuge was started as soon as an optical density of 1.5 was reached. The wet cell paste (800 g) was stored at −20 °C.

Purification of Glycolate Oxidase. Yeast cell paste (200 g) was thawed and suspended in 0.1 M Tris buffer, 1 mM EDTA, 10 μM PMSF, and 0.1 mM FMN, pH 8.5 (100 mL). The cell suspension was subjected to 6 times 1-min cell breakage in a bead beater (Biospec Products, Bartlesville, OK; Model 909) half-filled with 0.5-mm glass beads. The resulting slurry (about 350 mL) was centrifuged for 1 h at 23300*g*. The supernatant was dialyzed against two changes (6 L each) of 5 mM Tris buffer, pH 8.3, containing EDTA, PMSF, and FMN in the same concentration as mentioned above. The dialyzate was loaded on a hydroxyapatite column (20 × 8 cm, consisting of a 500-mL suspension of Bio-gel HT from Bio-Rad and 100 g of cellulose CF 11 from Whatman) and washed thoroughly with the same buffer until the absorbance at 280 nm fell below 1. The column was washed with 500 mL of 20 mM potassium phosphate buffer, pH 8.3, and finally with a gradient of 500 mL of 200 mM potassium phosphate introduced into 500 mL of 20 mM potassium phosphate buffer, pH 8.3. The peak of the glycolate oxidase activity is found at 0.1 M potassium phosphate. The active fractions were pooled, and solid ammonium sulfate was added to give 50% saturation. The precipitated protein was collected by centrifugation at 23300*g* for 30 min. The pellet was dissolved and then dialyzed against two changes (1 L each) of 5 mM Tris buffer, pH 8.3, and the dialyzate was loaded on a column of Q-sepharose (50 × 3 cm) and washed with the same buffer. Glycolate oxidase activity is found in the first protein-containing fractions. The active fractions were pooled and brought to 50% ammonium sulfate saturation. The purified enzyme is stored on ice as a suspension in 50% saturated ammonium sulfate, containing 0.1 mM free FMN.

Preparation of 8-Mercapto-FMN Glycolate Oxidase. Glycolate oxidase suspension was spun down and the pellet redissolved in 0.1 M potassium phosphate buffer, pH 8.3, containing a 4-fold excess of 8-mercapto-FMN (based on the concentration of enzyme bound FMN). The displacement of the native FMN with 8-mercapto-FMN can be followed spectrophotometrically by the increase in absorbance at 650 nm associated with enzyme-bound 8-mercapto-FMN and was complete after approximately 4 h (at 4 °C). The sample was then passed through a G-25 column to separate free 8-mercapto-FMN and released FMN from the protein. This protocol yielded 93% 8-mercapto-FMN glycolate oxidase.

Determination of the Extinction Coefficient. The extinction coefficient of glycolate oxidase in 0.1 M potassium phosphate, pH 8.3, was determined from the change in absorbance following the release of FMN by trichloroacetic acid (final concentration 5% v/v). The precipitated protein was spun down for 10 min at 17300*g* and the supernatant immediately neutralized with solid sodium carbonate. The extinction coefficient for FMN bound to glycolate oxidase was calculated on the basis of an extinction coefficient of 12 500 M^{-1} cm^{-1} for free FMN.

Photoreduction. Glycolate oxidase was made anaerobic by alternate evacuation and flushing with oxygen-free argon. The photochemical reduction, using EDTA and 5-deazariboflavin as catalyst, was then performed as described by Massey and Hemmerich (1978). Light irradiation was carried out with a sun gun (Smith Victor Corp., Griffith, IN) at an intensity of 6×10^6 erg s^{-1} cm^{-2}, if not stated otherwise.

Instrumentation. Absorbance spectra were recorded either with a Varian spectrophotometer, Cary Model 219, or with a Hewlett Packard diode array spectrophotometer, Model 8452A. Excitation and emission spectra were recorded with a ratio recording instrument designed and built by Dr. D. P. Ballou and Mr. G. Ford (University of Michigan). Rapid reaction studies were carried out in a temperature-controlled stopped-flow apparatus interfaced with a Nova 2 (Data General) computer system (Beaty & Ballou, 1981). The observation path of the cell was 2 cm.

Steady-state kinetics of glycolate oxidase were studied also in the stopped-flow instrument by monitoring the absorbance changes at 450 nm with time (enzyme-monitored turnover). The obtained data were analyzed according to the method

Table I: Purification of Yeast-Derived Spinach Glycolate Oxidase

purification step	volume (mL)	protein content[b] (mg/mL)	units[c]	sp act. (units/mg)	yield (%)	purification (*n*-fold)
(I) crude extract[a]	350	265	0.7	0.0026	100	1
(II) dialysis	380	224	0.48	0.0021	74	0.8
(III) hydroxyapatite (pool)	750	2.7	0.21	0.078	64	30
(IV) Q-Sepharose (pool)	140	0.23[d]	0.83	3.6	47	1384

[a] From 200 g of wet yeast cell paste. [b] Protein content was estimated by assuming that an A_{280} of 1 equals 1 mg/mL protein. [c] Units were determined by using an enzyme-coupled assay as described under Materials and Methods. [d] Yield of glycolate oxidase was typically between 12 and 14 mg.

described by Gibson et al. (1964).

Results

Expression and Purification of Glycolate Oxidase. Previous attempts to express glycolate oxidase in *Escherichia coli* cells yielded inactive and insoluble enzyme (data not shown). We therefore constructed plasmid *p*GAO (see Figure 1), which expresses active, soluble glycolate oxidase in the baker's yeast *Saccharomyces cerevisiae*. Furthermore, the active enzyme can be isolated from yeast cells transformed with *p*GAO and grown in large quantities (180 L).

The purification method described here takes advantage of (a) binding of the enzyme to hydroxyapatite and (b) lack of binding to anion exchangers, such as DEAE or Q-Sepharose, due to its very high isoelectric point (>9.6; Kerr & Groves, 1975). The high affinity of glycolate oxidase and hydroxyapatite was first employed by Zelitch and Ochoa (1953) in an attempt to purify the enzyme from spinach. Kerr and Groves (1975) used a different protocol to purify the enzyme from *Pisum sativum* leaves with their major step being DEAE chromatography. These authors estimated the p*I* of glycolate oxidase to be above 9.6. A combination of these two steps proved to be an efficient procedure for the purification of spinach glycolate oxidase expressed in baker's yeast.

Glycolate oxidase was purified approximately 1400-fold from yeast cells, indicating that glycolate oxidase accounts for 0.07% of the soluble protein. Details of the purification procedure are given in Table I. The A_{274}/A_{448} ratio, which can be used as a criterion for purity, was found to be 8.8, slightly higher than the value of 7.4 for the spinach enzyme (Zelitch & Ochoa, 1953; Frigerio & Harbury, 1958). Analysis of the purified enzyme by SDS gel electrophoresis showed only minor impurities which accounted for less than 2% of the total protein.

Stability and Storage of Glycolate Oxidase. Purified glycolate oxidase was found to lose activity when stored in 0.1 M potassium phosphate/0.3 mM EDTA, pH 8.3 and 2 °C. The loss of activity is associated with an increase of fluorescence, suggesting that FMN is irreversibly released from the (nonfluorescent) enzyme. Attempts to reconstitute the protein in the presence of high concentrations of FMN (1 mM) and reducing agent (1 mM DTT) were not successful. However, the activity of the enzyme can be preserved in an ammonium sulfate suspension, pH 8.3, containing 0.1 mM FMN (Frigerio & Harbury, 1958) or alternatively in 50% ethylene glycol at −20 °C (Kerr & Groves, 1975). For practical reasons, we chose the former method to store glycolate oxidase.

Spectral Properties of Glycolate Oxidase. The absorption spectrum of glycolate oxidase is shown in Figure 2. The absorbance maxima are at 346 and 448 nm. Similar values have been reported by Frigerio and Harbury (1958) for the spinach enzyme and for glycolate oxidase isolated from pea leaves and pumpkin cotyledons [see Fendrich and Ghisla (1982) and Nishimura et al. (1983), respectively]. The unusual bathochromic shift of the near-UV peak from 373 nm in free flavin to 346 nm in protein-bound FMN was taken as evidence that the N(3) position of the enzyme-bound flavin is deprotonated (p*K* for free flavin is 10.3). This phenomenon will be described in more detail in a later section.

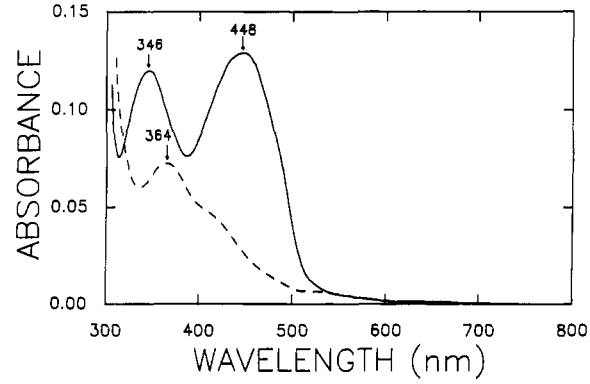

FIGURE 2: Absorbance spectra of glycolate oxidase in the oxidized and reduced states. The solid trace shows the absorbance spectrum of oxidized glycolate oxidase (13.4 μM) in 20 mM Tris buffer, pH 8.3. After anaerobiosis was established, 10 μL of 0.1 M glycolate was mixed with the enzyme, and the reduced spectrum (dashed trace) was recorded.

The extinction coefficient at 448 nm in 0.1 M potassium phosphate at pH 8.3 and 4 °C was determined to be 9200 M^{-1} cm^{-1} (see Materials and Methods).

Anaerobic reduction with substrate (glycolate or glyoxylate) gives rise to an absorption spectrum with a peak at 364 nm as is shown in Figure 2.

After removal of free flavin by gel chromatography (G-25) or exhaustive dialysis, glycolate oxidase exhibits no fluorescence. The substrate-reduced enzyme, however, is slightly fluorescent with an excitation spectrum maximal at 370 nm, closely similar to the absorption spectrum maximum (see Figure 2). Similar observations have been reported for the closely related lactate oxidase (Ghisla et al., 1974).

Oxalate Binding. Zelitch and Ochoa (1953) as well as Frigerio and Harbury (1958) reported that only glycolate and L-lactate, but not glyoxylate, reduce spinach glycolate oxidase. A few years later, Richardson and Tolbert (1961) demonstrated that glyoxylate also serves as a substrate for glycolate oxidase and that the failure to detect oxidation of glyoxylate was due to the inhibitory effect of oxalate, present in the crude extracts used in the earlier investigations. Recently, Nishimura and co-workers (Nishimura et al., 1983) determined a K_i value of 4.3 mM (35 °C) for the inhibition by oxalate of glycolate oxidase isolated from pumpkin cotyledons. We found inhibition constants of K_i = 2.8 and 0.21 mM for the spinach enzyme at 25 and 4 °C, respectively. At both temperatures, standard kinetic analysis (Segel, 1975) indicated partial competitive inhibition.

Binding of oxalate was also studied spectrophotometrically by titrating the enzyme with oxalate (Figure 3). The observed

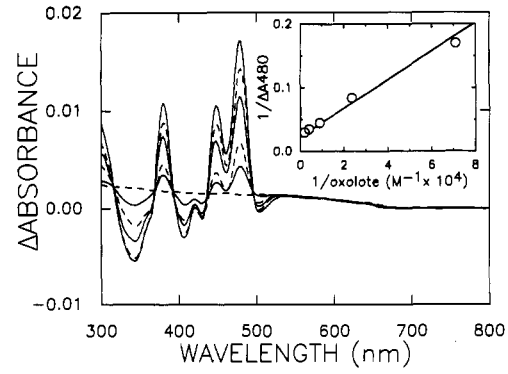

FIGURE 3: Titration of glycolate oxidase with oxalate in 0.1 M potassium phosphate buffer, pH 7.3, 4 °C. Difference spectra were recorded after addition of oxalate to 0 μM (dashed trace), 14 μM (solid trace), 42.6 μM (dashed trace), 113.8 μM (solid trace), 254 μM (dashed trace), and 525 μM (solid trace) to the glycolate oxidase solution in the sample cuvette. The same volume of buffer was added to the same concentration and volume of glycolate oxidase solution in the reference cuvette. Inset: Benesi–Hildebrandt plot ($1/\Delta A_{480}$ versus 1/[oxalate]) which yields a K_d of 8×10^{-5} M.

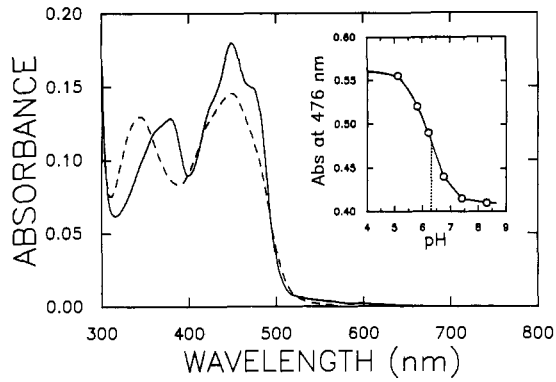

FIGURE 4: Comparison of the absorption spectrum of glycolate oxidase at pH 5 (solid trace) and pH 8.3 (dashed trace). Both spectra were recorded in 20 mM Tris buffer at 4 °C. The inset shows data obtained from a pH titration of glycolate oxidase: the pH was increased stepwise by small additions of solid sodium carbonate.

spectral changes allowed calculation of the dissociation constant of 8×10^{-5} M at pH 7.3 (see inset of Figure 3) and a slightly higher value of 2.4×10^{-4} M at pH 8.3. This statically determined value (K_d = 0.24 mM) matches very nicely the inhibition constant (K_i = 0.21 mM)) measured in the steady-state experiments carried out at pH 8.3, 4 °C, and described in the previous paragraph. Binding of oxalate to glycolate oxidase is markedly different from lactate oxidase both in terms of the spectral changes observed (Ghisla & Massey, 1977; Figure 1) and also in terms of the dissociation constant, which is substantially lower for lactate oxidase (K_d = 1.6×10^{-5} M; Ghisla & Massey, 1974). Moreover, light irradiation of the glycolate oxidase–oxalate complex did not result in formation of a photoadduct as is the case for lactate oxidase (Ghisla et al., 1979).

pH Dependence of the Absorption Spectrum. Glycolate oxidase shows a marked dependence of its absorption spectrum on the pH, as documented in Figure 4. At pH 5, the absorption peak at 448 nm is nicely resolved, and the near-UV peak is positioned at 375 nm, whereas at pH 8.3 both peaks are unresolved and the near-UV peak is shifted to lower wavelengths (346 nm). The features of the absorption spectra as well as the nature of the spectral changes clearly indicate that FMN bound to glycolate oxidase is deprotonated at the N(3) position at pH 8.3. Since free oxidized FMN exhibits a pK_a of 10.3, it is clear that glycolate oxidase lowers the pK_a of the bound FMN by several pH units. A pH titration of

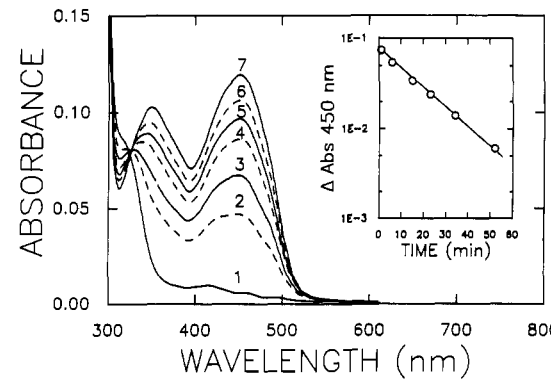

FIGURE 5: Determination of sulfite dissociation (k_{off}) with MMTS. Glycolate oxidase (13 μM) in 1 mL of 0.1 M potassium phosphate, pH 8.3 at 4 °C, was reacted with 6 μL of 1 M sodium sulfite and concentrated in a Centricon microconcentrator to 100 μL in order to remove excess sulfite. The sample was rediluted to 1 mL and a spectrum recorded (spectrum 1). Ten microliters of 0.1 M MMTS solution was now added, and the reappearance of the oxidized glycolate oxidase was followed with time. The spectra shown were recorded after 1 (spectrum 2), 6.5 (spectrum 3), 15 (spectrum 4), 23 (spectrum 5), and 34 min (spectrum 6). After no further spectral changes occurred, spectrum 7 was recorded. The inset shows a semilogarithmic plot of the spectral changes at 450 nm versus time. From this plot, a half-life of 14.5 min (k_{off} = 8.25×10^{-4} s^{-1}) can be calculated.

the enzyme (see Figure 4, inset) reveals that the pK_a of the bound FMN is shifted to approximately pH 6.4, i.e., by 4 pH units. Similar observations were made for other plant glycolate oxidases, although pK_a values have not been reported (Nishimura et al., 1983; Fendrich & Ghisla, 1982), and for the enzyme isolated from pig kidneys (Schuman & Massey, 1971a) which has a pK_a of 8. It is therefore conceivable that glycolate oxidases from all sources share the property of substantially lowering the pK of the flavin N(3)H.

The low extinction coefficient (9200 M^{-1} cm^{-1} at pH 8.3) reported above is in keeping with a deprotonated flavin species since free FMN also shows a decrease of its absorption at 444 nm upon deprotonation of the N(3) position. On the basis of the extinction coefficient at pH 8.3, an extinction coefficient of 11 500 M^{-1} cm^{-1} can be calculated for the protonated species at pH 5, a value well within the range of extinction coefficients determined for other flavoproteins.

Stabilization of a Negative Charge at the Flavin N(1)-C(2=O) Locus. Upon reduction of flavoprotein oxidases with substrate (or other reductants), the reduced flavin ring system appears to be present in its anionic form [N(1) deprotonated]. It is thought that a positively charged amino acid side chain (like an arginine or lysine) stabilizes the negative charge in the flavin N(1)–C(2=O) locus, thereby enhancing the nucleophilicity of the N(5) position, which serves as an entry port for electrons. Three pieces of evidence support this model: (a) formation of tight sulfite adducts; (b) stabilization of the anionic flavin semiquinone; and (c) stabilization of the benzoquinoid form of 8-mercaptoflavin [see Ghisla and Massey (1986) for a review]. In the following sections, we will demonstrate that all three criteria are fulfilled for glycolate oxidase.

Formation of a Reversible Sulfite Adduct. Glycolate oxidase forms a flavin N(5)-sulfite adduct, with almost complete loss of the 448-nm absorbance band (cf. Figure 5). Titration with sulfite revealed that binding was too tight to obtain a reliable value for the dissociation constant. Therefore, we determined the dissociation constant kinetically by mixing glycolate oxidase with sulfite in the stopped-flow instrument. At all concentrations of sulfite, the loss of absorbance at 448 nm is a single-exponential process, and from the slope of the linear plot of the measured k_{app} versus the sulfite concentration,

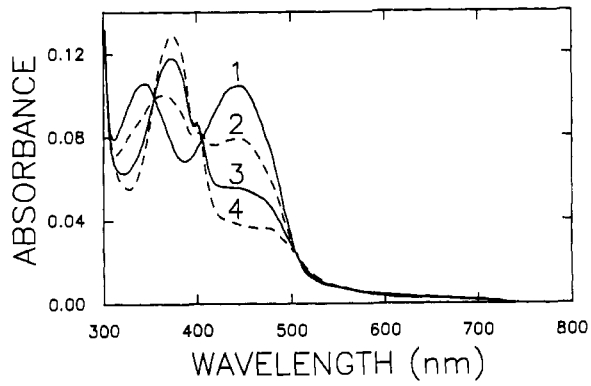

FIGURE 6: Photoreduction of glycolate oxidase; 11.4 μM glycolate oxidase in 20 mM Tris buffer, pH 8.3 (1 mL) at 4 °C, was made anaerobic by repeated cycles of evacuation and flushing with oxygen-free argon and subsequently mixed with 15 μL of 0.3 M EDTA solution and 0.5 μL of 10^{-3} M 5dRfl solution. The spectra shown were recorded after irradiation with a sun gun (see Materials and Methods) for 0 s (trace 1), 20 s (trace 2), 60 s (trace 3), and 15 min (trace 4).

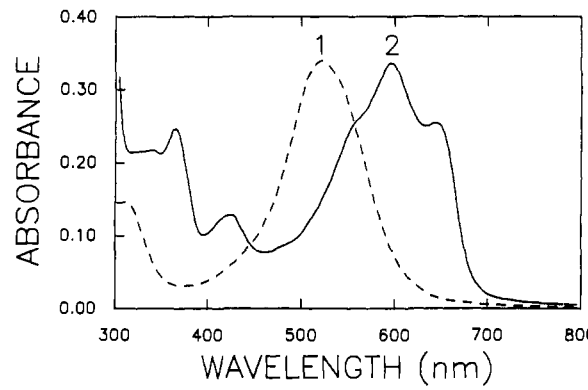

FIGURE 7: Comparison of the absorption spectrum of 8-mercapto-FMN and 8-mercapto-FMN glycolate oxidase. The dashed trace shows the spectrum of free 8-mercapto-FMN in 0.1 M potassium phosphate, pH 8.3 at 4 °C. The solid trace shows the spectrum of 8-mercapto-FMN glycolate oxidase under the same conditions. 8-Mercapto-FMN glycolate oxidase was prepared as described under Materials and Methods. The two spectra were normalized to the same absorbance at their wavelength maxima of 520 and 598 nm, respectively.

we calculated a value of 3100 M^{-1} s^{-1} for the association step (k_{on}). A value for k_{off} cannot be obtained from the same kinetic data since the plot of k_{app} versus sulfite concentration appears to go through the origin, indicating that k_{off} is very small. However, k_{off} can be measured by adding an excess of MMTS to the enzyme–sulfite complex. MMTS reacts rapidly with free sulfite, thus removing it from the equilibrium. The reappearance of the oxidized glycolate oxidase spectrum, which is independent of the MMTS concentration, can be followed spectrophotometrically and shows monophasic behavior with a half-life of 14 min (k_{off} = 0.825 × 10^{-3} s^{-1}) (see Figure 5, inset). Thus, we can calculate a value of 2.7 × 10^{-7} M at pH 8.3, 4 °C, for the dissociation constant K_d ($=k_{off}/k_{on}$), which is not as tight as for lactate oxidase (5.6 × 10^{-8} M at 25 °C) but tighter than for other flavoprotein oxidases (Ghisla & Massey, 1991).

Stabilization of the Anionic Flavin Semiquinone. Photoreduction of glycolate oxidase generated the red flavin semiquinone with absorbance maxima at 372 and 402 nm with a broad peak around 480 nm (Figure 6). The wavelength maxima as well as the increase of optical density at 372 nm can be regarded as a typical flavoprotein oxidase radical phenotype. Further reduction to the two-electron-reduced flavin was not observed probably due to the inability of the negatively charged deazaflavin radical to reduce a negatively charged flavin semiquinone radical (Massey & Hemmerich, 1978). This was also reported for lactate oxidase and glucose oxidase.

8-Mercapto-FMN Glycolate Oxidase. Earlier observations indicated that FMN is not bound very tightly to glycolate oxidase (Zelitch & Ochoa, 1953; Frigerio & Harbury, 1958). The ease with which FMN can be displaced supports these observations. A 4-fold excess of 8-mercapto-FMN was sufficient to displace the native FMN quantitatively. These results are similar to those obtained with D-amino acid oxidase, where 8-mercapto-FAD was found to be bound more tightly than FAD, and where the latter could be displaced quantitatively with a small molar excess of 8-mercapto-FAD (Fitzpatrick & Massey, 1983). The absorbance spectrum obtained (Figure 7) has maxima at 598, 422, and 366 nm with a pronounced shoulder at 648 nm and is very similar to other 8-mercaptoflavoprotein oxidase spectra, in particular lactate oxidase (Massey et al., 1979). Therefore, we conclude that glycolate oxidase stabilizes the benzoquinoid form of 8-mercaptoflavin (Massey et al., 1979).

The 8-mercapto-FMN can also be used to probe the accessibility of the 8-position of the flavin ring system. The reaction with both MMTS (0.6 mM) and iodoacetamide (1.2 mM) is extremely slow ($t_{1/2}$ = 7 and 6 days at 4 °C, respectively), suggesting that the 8-position is not accessible to solvent-borne reagents. This finding is in agreement with the crystal structure which shows that the 8-position of the isoalloxazine ring is, like all of the benzene ring moiety buried in the protein (Lindqvist, 1989).

8-Mercapto-FMN glycolate oxidase shows a much lower affinity for sulfite which binds reversibly to form the 8-mercapto-FMN, N(5)-sulfite adduct with a K_d of 125 mM at 4 °C. In common with other flavoprotein oxidases, formation of the 8-sulfonate flavin does not occur (Fitzpatrick & Massey, 1983). Like lactate oxidase and D-amino acid oxidase, 8-mercapto-FMN glycolate oxidase was not reduced by substrate (glycolate). In summary, 8-mercapto-FMN glycolate oxidase behaves in all respects like other 8-mercaptoflavoprotein oxidases, most notably its close relative lactate oxidase.

Steady-State Kinetics. Glycolate oxidase (8.5 μM) was mixed with glycolate (1–25 mM in 0.1 M potassium phosphate buffer, pH 8.3 and 4 °C) using a stopped-flow apparatus, and the decrease in optical density at 448 nm was monitored. The traces obtained from these enzyme-monitored turnover experiments were used to calculate the apparent turnover number at various oxygen concentrations (Gibson et al., 1964). Lineweaver–Burk plots for various glycolate concentrations yield a family of parallel lines (Figure 8). From the data shown in Figure 8, a K_m value of 0.2 mM for oxygen can be calculated. The turnover number (TN) at infinite glycolate concentration and the K_m for glycolate can be determined by replotting 1/apparent TN versus 1/[glycolate]. Values of 20 s^{-1} for TN and 1 mM for the K_m of glycolate are obtained.

The same steady-state experiment was also performed in Tris buffer (0.1 M Tris-HCl, pH 8.3 and 4 °C; data not shown). The analysis revealed that neither the TN nor the K_m for oxygen was altered whereas the K_m for glycolate was much higher (K_m = 5.2 mM). This finding supports earlier observations by Richardson and Tolbert (1961) that Tris buffer is a competitive inhibitor of the substrate.

Reductive Half-Reaction. Under anaerobic conditions, glycolate oxidase is rapidly reduced by glycolate, showing saturation at higher glycolate concentrations. This behavior

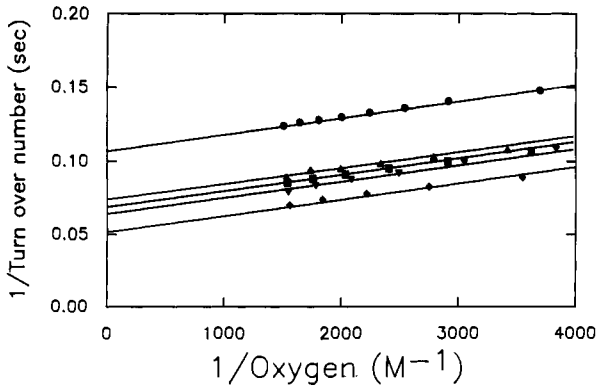

FIGURE 8: Steady-state kinetics of glycolate oxidase. Glycolate oxidase (14 μM) in air-saturated (21% oxygen) 0.1 M potassium phosphate buffer, pH 8.3 at 4 °C, was mixed with various glycolate concentrations in the same buffer equilibrated with 50% oxygen at 4 °C. The concentrations used (after mixing) were 1 (circles), 2 (triangles), 4 (squares), 10 (inverted triangles), and 25 mM (diamonds). Double-reciprocal plots of the apparent turnover number versus the oxygen concentration are shown.

indicates that the reduction step is essentially irreversible, following after the reversible equilibrium formation of a complex between oxidized enzyme and substrate (Strickland et al., 1975):

$$EFl_{ox} + \text{glycolate} \underset{k_2}{\overset{k_1}{\rightleftharpoons}} EFl_{ox}\text{–glycolate} \xrightarrow{k_3} EFl_{red}\ (+\text{glyoxylate})$$

A double-reciprocal plot of $1/k_{obs}$ versus 1/[glycolate] yields a straight line with a y intercept ($=1/k_3$) of 0.04 s (k_3 = 25 s^{-1}). The K_d for glycolate as derived from this double-reciprocal plot (slope divided by y intercept) is 0.94 mM, i.e., the same value as found for the K_m in the steady-state analysis. It should be noted that the rate of reduction (k_3 = 25 s^{-1}) is on the order of the maximal TN derived from the steady-state data described above, consistent with reduction of glycolate being the rate-limiting step in the catalytic turnover.

We also studied the reductive half-reaction in Tris buffer (0.1 M Tris–HCl, pH 8.3 and 4 °C) in order to confirm the inhibitory effect of Tris on the glycolate oxidation as shown by the steady-state experiments. As was seen in phosphate buffer, the rate of reduction approached a limiting value with higher glycolate concentrations. However, a double-reciprocal plot gave a much higher K_d = 5.3 mM corresponding to the higher K_m value in this buffer. Consistent with competitive inhibition of glycolate, the y intercept was the same; i.e., the limiting rate of reduction (k_3) is unchanged.

Oxidative Half-Reaction. Glycolate oxidase (13.4 μM) was anaerobically reduced with a 2-fold excess of glycolate, and the reoxidation was studied by mixing the reduced enzyme with buffer, equilibrated with various oxygen concentrations. The re-formation of oxidized enzyme was monitored at 448 nm. The reaction showed a linear dependency on the oxygen concentration, and a plot k_{obs} versus $[O_2]$ passed through zero. The data fit a second-order reaction rate with $k = 8.5 \times 10^4$ M^{-1} s^{-1}.

Discussion

In spite of the comparatively low expression level of spinach glycolate oxidase in bakers' yeast, the enzyme can be isolated in sufficient quantities to study its basic properties. Although the yield and purification factor are less suitable than can be obtained directly from some plant sources (Kerr & Groves, 1975; Nishimura et al., 1983), the yeast system provides the unique opportunity to study structure/function relationships of amino acids in the active site by mutagenesis.

The yeast-derived spinach glycolate oxidase shows all the characteristic features of the flavoprotein oxidase family, such as stabilization of the anionic flavinsemiquinone and the benzoquinoid form of 8-mercapto-FMN, and formation of a tight flavin N(5)-sulfite adduct. These properties have been explained by the hypothesis of a positively charged amino acid side chain stabilizing the negative charge at the flavin N(1)–C(2=O) locus that is introduced in all the cases mentioned above (including reduction by substrate) (Massey et al., 1979; Ghisla & Massey, 1986). The X-ray structure of spinach glycolate oxidase clearly supports this explanation: a lysine side chain (K230) is located close to the flavin N(1) and C(2=O) positions and makes a strong interaction with both the nitrogen and the oxygen atom (Lindqvist & Brändén, 1989). In order to substantiate this hypothesis, replacement of the lysine by a neutral amino acid should abolish all of these characteristics and render the protein virtually inactive.

At this point, a more detailed comparison to the related lactate oxidase is appropriate. Although these two enzymes share many basic properties such as a similar subunit molecular weight, 40 282 for glycolate oxidase (Volokita & Somerville, 1987; Cederlund et al., 1988) and 42 613 for lactate oxidase (Giegel et al., 1990), oligomeric structure (octameric) (Sullivan et al., 1977; Lindqvist & Brändén, 1985), type of substrate (α-hydroxy acids), etc., there are also some intriguing differences. The first of these is in the kinetics. Glycolate oxidase appears to react in a true ping-pong mechanism, in which the substrate, either glycolate or L-lactate, is oxidized to the corresponding α-keto acid at the expense of enzyme–flavin reduction, and then released from the active site. The reduced enzyme then reacts with molecular oxygen in a second-order reaction to regenerate oxidized enzyme and free hydrogen peroxide:

$$EFl_{ox} + \text{glycolate} \underset{k_2}{\overset{k_1}{\rightleftharpoons}} EFl_{ox}\text{–glycolate} \underset{k_4}{\overset{k_3}{\rightleftharpoons}} EFl_{red}H_2 + \text{glyoxylate}$$

$$EFl_{red}H_2 + O_2 \xrightarrow{k_5} EFl_{ox} + H_2O_2$$

The initial rate equation for this simple mechanism is

$$v = \frac{V_{max}}{1 + K_{glycolate}/[\text{glycolate}] + K_{O_2}/[O_2]}$$

where

$$V_{max} = k_3$$

$$K_{glycolate} = (k_2 + k_3)/k_1$$

$$K_{O_2} = k_3/k_5$$

The validity of this mechanism is confirmed by comparison of the steady-state and rapid reaction kinetics studies. From Figure 8, V_{max} = 20 s^{-1}, $K_{glycolate}$ = 1 × 10^{-3} M, and K_{oxygen} = 2.1 × 10^{-4} M. From the rapid reaction studies, k_3 was determined as 25 s^{-1}, k_5 as 8.5 × 10^4 M^{-1} s^{-1}, and the ratio k_2/k_1 ($=K_d$) as 9.4 × 10^{-4} M. If the formation of the enzyme–substrate complex is a rapid equilibrium event, i.e., $k_2 \gg k_3$, then $K_d = K_{glycolate}$, as observed. The predicted value of K_{oxygen} ($=k_3/k_5$) is 2.9 × 10^{-4} M, in reasonable agreement with the experimental value of 2.1 × 10^{-4} M.

By comparison, the kinetic mechanism of L-lactate oxidase is much more complex (Lockridge et al., 1972). The α-keto acid product, pyruvate, dissociates only slowly from the reduced enzyme, and the latter is not a component of the catalytic pathway. Instead, the reaction of molecular oxygen is with the reduced enzyme–pyruvate complex, and the resultant

Scheme I

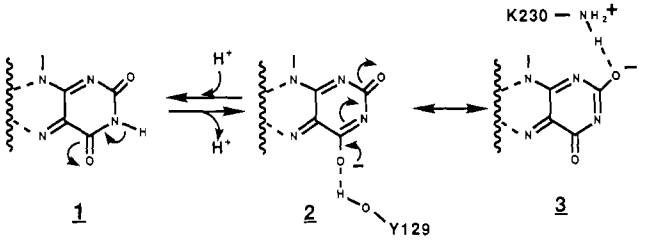

ternary complex of oxidized enzyme, pyruvate, and hydrogen peroxide is sufficiently stable for the peroxide to attack the keto acid to accomplish the oxidative decarboxylation typical of the enzyme, with acetate, carbon dioxide, and water as reaction products.

A further difference between the two enzymes is in their reaction with glycolate. Lactate oxidase has been shown to be able to abstract either the *re* hydrogen or the *si* hydrogen from glycolate with the subsequent formation of the corresponding enantiomeric flavin N(5)-glycolyl adducts; the former results in normal catalysis with formate, carbon dioxide, and water as final products, but the latter results in the formation of a stable flavin N(5)-glycolyl adduct (Massey et al., 1980; Ghisla & Massey, 1980). On the other hand, glycolate oxidase oxidizes glycolate to glyoxylate without any indication of the occurrence of such a catalytically incompetent adduct.

Finally, oxalate, which is believed to mimic the transiently formed carbanion species (Ghisla & Massey, 1977), binds much tighter (5–15 times) and with substantially different spectral changes to lactate oxidase than to glycolate oxidase. These differences suggest that the binding sites for substrate/product are significantly dissimilar, despite the impressive structural homology between the enzymes.

Another feature that sets the two enzymes apart is the low pK of the N(3) hydrogen of FMN bound to glycolate oxidase. Several factors can contribute to lower the pK_a of the N(3) hydrogen as depicted in Scheme I. The negative charge on N(3) can be delocalized to either C(2=O) or C(4=O). Both oxygen atoms form hydrogen bonds to a lysine and a tyrosine side chain, respectively, thereby stabilizing the deprotonated state of N(3). In addition, there is no interaction between the N(3) hydrogen and a hydrogen bond acceptor (an amino acid or water) which would counteract a facilitated deprotonation. pH titration performed with lactate oxidase showed that the pK is at least 9.5, i.e., unchanged or only slightly lowered compared to free flavin, again indicating that this part of the isoalloxazine ring system (i.e., the pyrimidine ring) experiences distinctly different environments in these two enzymes. However, Giegel et al. (1990) found that all of the amino acids thought to be involved in catalysis are highly conserved in lactate oxidase and glycolate oxidase (Giegel et al., 1990). Since structural data are not yet available for lactate oxidase, one can envision that conformational changes of the amino acids in the active site account for the observed differences. In other words, the orientation of the lysine and/or tyrosine may be such that the interactions depicted in Scheme I (structures **2** and **3**, respectively) cannot occur. Likewise, amino acids not yet identified may come into play in lactate oxidase which are not present in the active site of glycolate oxidase.

The low pK value of the oxidized flavin of spinach glycolate oxidase, obviously a common feature of glycolate oxidases in general, also has ramifications for the reduction of the flavin ring system: Since the pK for the N(3) hydrogen in the reduced state is much higher (>14; Macheroux et al., unpublished results), two-electron reduction of the isoalloxazine must be accompanied by protonation of the N(3) position. An obvious source for the proton is solvent water which has access to the active site via the same channel the substrate molecule travels through [see Lindqvist (1989)]. Another most intriguing possiblity is the abstraction of the hydrogen from the hydroxyl group of the tyrosine (Y129) which is very close to the N(3) position [distance between the oxygen of the tyrosine-129 side chain to N(3) is 3.38 Å] according to the crystal structure (Lindqvist, 1989). As a result, the nucleophilicity of the tyrosine oxygen would be enhanced, which in turn would facilitate the last step in catalysis, i.e., the breakdown of the N(5) adduct by means of abstraction of the α-hydroxy hydrogen.

In order to assign certain properties of the enzyme to specific amino acids in the active site, we will exchange the amino acids in question by site-directed mutagenesis and compare the properties of the mutant enzymes to the wild-type enzyme.

Acknowledgments

We thank Dr. C. R. Somerville for providing the cDNA clone of glycolate oxidase and for many helpful suggestions during the course of this work.

References

Ammerer, G. (1983) *Methods Enzymol. 101*, 192–201.
Beaty, N. B., & Ballou, D. P. (1981) *J. Biol. Chem. 256*, 4611–4518.
Cederlund, E., Lindqvist, Y., Söderlund, G., Brändén, C.-I., & Jörnvall, H. (1988) *Eur. J. Biochem. 173*, 523–530.
Fendrich, G., & Ghisla, S. (1982) *Biochim. Biophys. Acta 702*, 242–248.
Fitzpatrick, P. F., & Massey, V. (1983) *J. Biol. Chem. 258*, 9700–9705.
Frigerio, N. A., & Harbury, H. A. (1958) *J. Biol. Chem. 231*, 135–157.
Ghisla, S., & Massey, V. (1974) *J. Biol. Chem. 250*, 577–584.
Ghisla, S., & Massey, V. (1977) *J. Biol. Chem. 252*, 6729–6735.
Ghisla, S., & Massey, V. (1980) *J. Biol. Chem. 255*, 5688–5696.
Ghisla, S., & Massey, V. (1986) *Biochem. J. 239*, 1–12.
Ghisla, S., & Massey, V. (1991) in *Chemistry and Biochemistry of Flavoenzymes* (Müller, F., Ed.) Vol. II, CRC Press, Boca Raton, FL.
Ghisla, S., Massey, V., Lhoste, J.-M., & Mayhew, S. G. (1974) *Biochemistry 13*, 589–597.
Ghisla, S., Massey, V., & Choong, Y. S. (1979) *J. Biol. Chem. 254*, 10662–10669.
Gibson, Q. H., Swoboda, B. E. P., & Massey, V. (1964) *J. Biol. Chem. 239*, 3927–3934.
Giegel, D., Williams, Ch. Jr., & Massey, V. (1990) *J. Biol. Chem. 265*, 6626–6632.
Ito, H., Fukada, Y., Murata, K., & Kimura, A. (1983) *J. Bacteriol. 153*, 163–168.
Kerr, M. W., & Groves, D. (1975) *Phytochemistry 14*, 359–362.
Lindqvist, Y. (1989) *J. Mol. Biol. 209*, 151–166.
Lindqvist, Y., & Brändén, C.-I. (1985) *Proc. Natl. Acad. Sci. U.S.A. 82*, 6855–6859.
Lindqvist, Y., & Brändén, C.-I. (1989) *J. Biol. Chem. 264*, 3624–3628.
Lockridge, O., Massey, V., & Sullivan, P. A. (1972) *J. Biol. Chem. 247*, 8097–8106.
Maniatis, T., Fritsch, E. F., & Sambrook, J. (1982) *Molecular cloning: A Laboratory Manual*, Cold Spring Harbor

Laboratory Press, Cold Spring Harbor, NY.
Massey, V., & Hemmerich, P. (1978) *Biochemistry 17*, 9–17.
Massey, V., Ghisla, S., & Moore, E. G. (1979) *J. Biol. Chem. 254*, 9640–9650.
Massey, V., Ghisla, S., & Kieschke, K. (1980) *J. Biol. Chem. 255*, 2796–2806.
McKnight, G. L., & McConaughy, B. L. (1983) *Proc. Natl. Acad. Sci. U.S.A. 80*, 4412–4416.
Nishimura, M., Akhmedov, Y. D., Strazalka, K., & Akazawa, T. (1983) *Arch. Biochem. Biophys. 222*, 397–402.
Richardson, K. E., & Tolbert, N. E. (1961) *J. Biol. Chem. 236*, 1280–1284.
Schuman, M., & Massey, V. (1971a) *Biochim. Biophys. Acta 227*, 500–520.
Schuman, M., & Massey, V. (1971b) *Biochim. Biophys. Acta 227*, 521–537.
Schwam, H., Michelson, S., Randall, W. C., Sondey, J. M., & Hirschmann, R. (1979) *Biochemistry 18*, 2828–2833.
Segel, I. H. (1975) *Enzyme Kinetics*, pp 161–166, Wiley, New York.
Sherman, F., Fink, G. R., & Hicks, J. B. (1983) *Methods in yeast genetics*, Cold Spring Harbor Laboratory Press, Cold Spring Harbor, NY.
Strickland, S., Palmer, G., & Massey, V. (1975) *J. Biol. Chem. 250*, 4048–4052.
Sullivan, P. A., Choong, Y. S., Schreurs, W. J., Cutfield, J. F., & Shepherd, M. G. (1977) *Biochem. J. 165*, 357–383.
Thiele, D. J., Walling, M. J., & Hamer, D. H. (1986) *Science 231*, 854–856.
Tolbert, N. E., Clagett, C. O., & Burris, R. H. (1949) *J. Biol. Chem. 181*, 905–914.
Volokita, M., & Somerville, C. R. (1987) *J. Biol. Chem. 262*, 15825–15828.
Zelitch, I., & Ochoa, S. (1953) *J. Biol. Chem. 201*, 707–718.

Direct Measurement of Intramolecular Electron Transfer between Type I and Type III Copper Centers in the Multi-Copper Enzyme Ascorbate Oxidase and Its Type II Copper-Depleted and Cyanide-Inhibited Forms†

T. E. Meyer,‡ A. Marchesini,§ M. A. Cusanovich,‡ and G. Tollin*,‡

Department of Biochemistry, University of Arizona, Tucson, Arizona 85721, and Istituto Sperimentale per la Nutrizione Delle Piante, Sezione-Torino, 10125 Torino, Italy

Received November 14, 1990; Revised Manuscript Received February 8, 1991

ABSTRACT: Transient kinetics of reduction of zucchini squash ascorbate oxidase (AO) by lumiflavin semiquinone have been studied by using laser flash photolysis. Second-order kinetics were obtained for reduction of the type I copper with a rate constant of 2.7×10^7 M^{-1} s^{-1}, which is comparable to that obtained with other blue copper proteins such as plastocyanin. Following reduction, the type I copper was reoxidized in a protein concentration independent (i.e., intramolecular) reaction (k_{obs} = 160 s^{-1}). Comparison with literature values for limiting rate constants in transient single-turnover kinetic experiments suggests that intramolecular electron transfer probably is the rate-limiting step in enzyme catalysis. The extent of reoxidation of type I copper was approximately 55%, which is consistent with the approximately equal redox potentials of the type I and type III copper centers. Neither azide nor fluoride caused any significant changes in kinetics, although they are enzyme inhibitors and are thought to bind to the type II copper. In contrast, cyanide caused a concentration-dependent decrease in the extent of intramolecular electron transfer (with no change in rate constant), and decreased the rate constant for reduction of the type I copper by a factor of 2. The apparent dissociation constant for cyanide (0.2–0.4 mM) is similar to that reported for inhibition of enzyme activity. Removal of the type II copper from AO only marginally affected the kinetics of electron transfer to type I copper ($k = 3.2 \times 10^7$ M^{-1} s^{-1}) and slightly increased the extent but did not alter the rate constant of intramolecular electron transfer. This provides a direct confirmation that type III copper is the immediate electron acceptor from type I copper. Cyanide also inhibits intramolecular electron transfer in type II copper-depleted protein just as in the holoprotein, with a similar apparent dissociation constant. This suggests that cyanide binds to the type III copper center rather than to type II copper.

The blue copper oxidases are widespread in plants, animals, and fungi (Dawson, 1966; Reinhammar & Malmström, 1981; Kroneck et al., 1982). They are large molecular weight soluble proteins which couple the oxidation of small molecules such as phenols and ascorbate to reduction of molecular oxygen. They contain a minimum of four copper atoms which represent three copper environments per subunit. The three-dimensional structure of zucchini squash ascorbate oxidase has been determined (Messerschmidt et al., 1989) and serves as the prototype for all the blue oxidases, whose sequences have been aligned on the basis of folding patterns and residues necessary for binding the copper atoms (Messerschmidt & Hüber, 1990). Ascorbate oxidase exists as a dimer of 70-kDa subunits, each of which folds in three interacting domains. The type I or blue copper has an absorption maximum at about 610 nm, and its binding site is similar to that in the small copper proteins azurin, plastocyanin, pseudoazurin, and cucumber basic blue protein, for which there are also three-dimensional structures.

† This work was supported in part by grants from the National Institutes of Health (DK15057 to G.T. and GM21277 to M.A.C.).
* To whom correspondence should be addressed.
‡ University of Arizona.
§ Istituto Sperimentale per la Nutrizione Delle Piante.

0006-2960/91/0430-4619$02.50/0